Selective catalytic reduction of NO_x with NH_3 using ZSM5 with low content of copper

L. Sandoval Rangel, C.J. Lucio-Ortiz, J. Rivera de la Rosa[*,β]
Facultad de Ciencias Químicas, Universidad Autónoma de Nuevo León
San Nicolás de los Garza, Nuevo León, 64451, México.

[β] *Centro de Innovación, Investigación y Desarrollo en Ingeniería y Tecnología,*
Universidad Autónoma de Nuevo León. Apodaca, Nuevo León, 66600, México.

M.J. Castaldi
The City College of New York, City University of New York
New York City, NY, 10031, U.S.A.
(Received: July 5th, 2015; Accepted: February 9th, 2016)

A comprehensive experimental and characterization study of selective catalytic reduction of NO_x with NH_3 was carried out on Cu-ZSM5 catalysts, previously prepared by the aqueous ion exchange method with a copper loading of 0.2, 1 and 2 %. Results showed that even with Cu contents as low as 2 % over zeolite, NO_x conversions higher than 92 % are obtained at 600 ºC. The copper catalysts were characterized using FT-IR, XRD, UV-Visible and with studies such as SEM, STEM and HRTEM, where the presence of CuO cores were shown to enhance the de-NO_x activity, due to their higher thermal stability compared with the other copper species found. The predominance of dispersed 4-5 nm particles over the zeolite was identified, which accounts for the high NO_x conversion results shown in SCR process.

Keywords: Selective catalytic reduction, ZSM-5, NO_x, Ammonia

Introduction

Due to a number of important advantages, like an increased efficiency, a lower cost and lower hazard issues, diesel has rised as one of the most used fossil fuels [1,2]. However, nitrogen oxides (NO_x) emission is a problem, since this pollutant is more complicated to eliminate from diesel exhaust emissions [3,4]. Nitrogen oxides (defined as the sum of NO and NO_2 gases) are major air pollutants generated by anthropogenic activities, with some of their harmful effects on humans and the environment being tropospheric ozone production [5,6], acid rain contribution [7,8], and formation of carcinogenic particles [9,10].

Vehicles are one of the main sources of NO_x, emitting between 81 and 88 % of the total amount of this pollutant in the principal 5 Mexican metropolitan areas in 2005, with the notable exception of Monterrey City [11]. However, in the biggest Mexican cities the increase of automobile circulation has been evident. Monterrey and Mexico City show the highest number of vehicles in Mexico, with 2.3 and 5.5 million units circulating by 2014 [12-14].

In the last decade, NO_x conversion using Selective Catalytic Reduction (SCR) has been proposed and studied thoroughly, in order to address the more strict legislation concerning pollutants emissions from diesel engines, which range from 0.04 g/km in the US, to 0.08 and 0.12 g/km in the EU and Mexico, respectively [15,16].

Two different SCR variations have been proposed; one in which hidrocarbons are used as NO_x reductants (HC-SCR), and another where NH_3 is using as the main reducing agent (NH_3-SCR). However, due to problems involved with use of hidrocarbons as reductants, like increase of fuel consumption, higher hydrocarbon emissions to the environment, and technical problems with application of catalysts in these type of systems, HC-SCR has not been yet extensively applied in diesel vehicles [4]. On the other hand, NH_3-SCR is the most used and commercially applied variation, with an aqueous solution of 32.5 wt% urea most often used as the NH_3 source for SCR in diesel vehicles due to its safer nature compared with gaseous ammonia [17].

SCR de-NO_x mechanisms depend strongly on NO/NO_2 proportion [18]. NO_x in diesel exhaust of light-duty engines usually consists of more than 90 % NO and only a small fraction of NO_2 (10 %); therefore, "standard" SCR reaction regularly takes place [19]:

$$4NH_3 + 4NO + O_2 \rightarrow 4N_2 + 6H_2O \quad (1)$$

However, if NO_2 proportion is excessive (NO_2 > 50 % of NO_x), nitrogen dioxide and ammonia react according to the reaction:

$$4NH_3 + 3NO_2 \rightarrow 3.5N_2 + 6H_2O \quad (2).$$

On the other hand, if $NO/NO_2 = 1$, the "fast" SCR reaction takes place [20, 21]:

$$4NH_3 + 2NO + 2NO_2 \rightarrow 4N_2 + 6H_2O \quad (3).$$

The SCR of NO_x with NH_3 has been studied extensively on diverse catalylsts, especially those consisting of vanadium, tungsten and titanium [22,23]. However, due to problems related with toxicity of vanadium and tungsten, along with low stability at high temperatures, metallic zeolites are being increasingly used for de-NO_x applications [24-26].

[*] *javier.riverad@uanl.edu.mx*

The most investigated zeolite material is Cu-ZSM5, since its catalytic potential discovery back in 1986 [27]. In general, Cu-zeolites have been reported as more active at lower temperatures than their Fe equivalents [28].

Though there are considerable studies on Cu-ZSM5 as catalyst for SCR of NO_x with NH_3, general focus has been given to high contents of metal in the zeolite, ranging from 3 to 5 % [29, 30, 32]. Therefore, the aim of this work was to evaluate the effect of low contents of Cu in the zeolite on the NO_x reduction capacity of the catalyst; this is important to analyze in order to evaluate the influence of Cu loading over zeolite, for SCR of NO_x, and also in order to optimize the use of this metal.

Materials and Methods

Cu-ZSM5 were all prepared by aqueous ion exchange of commercial NH_4-ZSM5 (Zeolyst CBV2314, Si/2Al = 23, surface area = 425 m^2/g) with the necessary $CuCl_2 \cdot 2H_2O$ (≥ 99.0 %, Sigma-Aldrich) in order to achieve metal contents of 0.2, 1.0 and 2.0 wt%. The ion exchange procedure was performed according to the methodology proposed by Kröcher *et al*. [31], which consisted on mixing the necessary amount of Cu salt in a suspension of ZSM5 zeolite in water. Afterwards, the resulting mixture was stirred over a heating plate (Fischer Scientific, model Isotemp 11-800-49SHP) at 80 ºC under nitrogen atmosphere for 12 hours. The mixture was then vacuum-filtered using a 2.5 μm paper, washing the filtered solid with 200 mL per gram of catalyst. The resulting material was then dried at 80 ºC (Thermo Scientific, model Lindberg Blue M) for 12 hours, and calcined at 500 ºC for 3 hours (Across, model TF1400). Blue powders were obtained. Finally, the catalysts were grinded on a porcelain mortar, and stored in glass vials at room temperature.

For the SCR of NO_x, a stainless steel reactor with a furnace was used. A gas mixture consisting of 1000 ppm NO, 1000 ppm NH_3 and 10 % air in balance of argon was introduced in the reactor. The total gas flow was 500 mL/min, obtaining a space velocity (GHSV) of 30,000 $cm^3h^{-1}g_{cat}^{-1}$. The catalytic performance was evaluated from 200 to 600 ºC, in 100 ºC steps, using a fresh catalyst for every experiment. The catalyst was packed between quartz wool inside the reactor. NO_x conversion was measured using a NO-NO_2-NO_x chemiluminescence analyzer (Thermo Electron, model 42i-HL), and an ammonia scrubber was adapted to the line before entering the NO_x analyzer, in order to avoid a decrease in instrument sensitivity [32]. For every experiment, a mixture of NO, air and argon was flowed through the reactor and the chemiluminescence analyzer for 30 minutes, in order to stabilize NO_x readings. After introducing NH_3 flow, the whole system was stabilized during 10 minutes.

After the SCR reaction, the catalysts were removed from the quartz wool packing using a stainless steel spatula, and in all cases, the used metallic zeolites were stored in glass vials at room temperature.

Metal composition was measured after acid digestion using an atomic absorption spectrophotometer (AAS, Thermo Scientific, model iCE 3400).

Table 1. Copper contents after modification of the ZSM5 zeolites with Cu.

Sample	Pretended Cu content (wt. %)	Experimental Cu content (wt. %)
Cu(0.2%)ZSM5	0.2	0.14
Cu(1%)ZSM5	1.0	0.86
Cu(2%)ZSM5	2.0	1.28

To monitor changes in characteristic vibrations of copper exchanged ZSM5, infrared spectra were recorded using FT-IR (Fisher Scientific, model Nicolet 6700). The samples were analyzed in the form of potassium bromide (KBr) solid disks, and the software used for analysis was OMNIC (Thermo Scientific), in transmittance mode. All FT-IR spectra consist of 32 scans and a resolution of 4 cm^{-1}.

The zeolite phases and crystallinity were evaluated using X-ray diffraction (Siemens, model D-5000). All samples were mounted on a glass holder. Each test was performed using the characteristic Cu Kα radiation in the 2θ range of 5 to 80º, with a 0.020º increase for every 4 seconds. All XRD tests were performed at room temperature.

The morphology and particle size studies for the fresh Cu(2%)ZSM5 catalyst were determined by scanning electron microscopy (SEM, JEOL, model JSM6701F), scanning transmission electron microscopy, high resolution transmission electron microscopy (STEM and HR-TEM, respectively, FEI, model Titan G2 30-800), and elemental analysis were performed using energy dispersive X-ray spectroscopy (EDS). The samples were placed on a support grid (lacey/carbon 200 mesh Cu) before the analysis.

In order to evaluate the copper oxidation state, UV-Visible spectroscopy (Thermo Electron, model Evolution 300) was used. All tests were performed in a wavelength range of 200 to 1000 nm, using the diffuse reflectance mode. The solid catalyst samples were compressed in 10 mm thick tablets before characterization with this instrument.

Results and Discussion

Table 1 summarizes copper content in the modified zeolites according to AAS. As observed, experimental Cu contents vary from 65 to 85 % from the originally intended copper loading; it has been previously reported that aqueous ion exchange of copper on zeolites presents a limitation, in which only about 50 % of the metal is exchanged in the support [18].

Figure 1 shows the selective catalytic reduction test results comparison Cu exchanged zeolites, for different contents in the catalysts. The experimental error from the tests was small, so it was omitted from the plot. Though high concentrations of metals (sometimes as high as 5 %) in zeolites have been recommended as having the best catalytic performance in the NH_3-SCR of NO_x [31], our results presented in Figure 1 have shown that even with low contents, a high SCR performance is achieved. Even with the lowest metal content (0.2 %), 61 % NO_x conversion was achieved (Cu-ZSM5) at 400 ºC, while by 500 ºC, this same

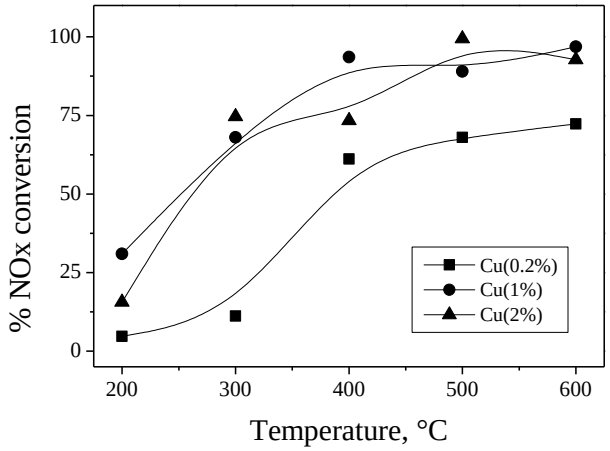

Figure 1. NO_x conversion versus temperature for ZSM5 zeolites modified with different Cu loadings.

catalyst showed a 68 % conversion. Cu(0.2%)ZSM5 had a more stable behavior at high temperatures; however, the NO_x conversion ability did not increase as much as in the 300-400 ºC step.

As expected, though, with higher metal content in the zeolite, the SCR performance increased. For Cu(1%)ZSM5, it is observed that a higher NO_x conversion is obtained when having only a 1.0 % metal content rather than 2.0 %. This could be due to a better metal dispersion over the catalyst, which leads to a higher catalytic activity. Cu-ZSM5 catalysts showed the highest NO_x conversion rates at temperatures above 500 ºC.

A fluctuation between 90 and 100 % conversion was observed at this temperature range, while Kröcher *et al.* has reported that, for a Cu-ZSM5 zeolite, a sharp decline in catalytic activity was observed at high temperatures, showing 67 % conversion at 500 ºC, 50 % at 550 ºC and 42 % at 600 °C, with a copper content of 2.9 %, and using reaction conditions very similar to the ones used in our study [31].

The FT-IR spectra of the fresh and used ZSM5 zeolites with 0.2 and 2 % copper content are shown in Figure 2. As is observed from the figure, FT-IR results were nearly identical for the different copper contents.

The whole vibration spectra corresponds clearly to the NH_4-ZSM5 zeolite; and though the broad signal from 3000 to 3700 cm^{-1} is related to the typical stretching bands of water, the shoulders presented in this region indicate the presence of structural OH groups [33, 34]. The bands at 3620 and 3450 cm^{-1} are assigned to ZSM5 O-H stretching modes, while the clear signal at 1400 cm^{-1} is due to N-H stretching and bending modes [35], likely related to some ammonium not exchanged and still present from the original NH_4-ZSM5 form. However, at 600 °C the conditions are too harsh for these species to persist over the zeolite and decomposes, which explains why at higher temperatures this signal disappears in both cases.

The bands below 1300 cm^{-1} are characteristic of NH_4-ZSM5. The signals at 1225 and 1070 cm^{-1} are assigned to asymmetrical stretching vibrations of tetrahedral Si-Al,

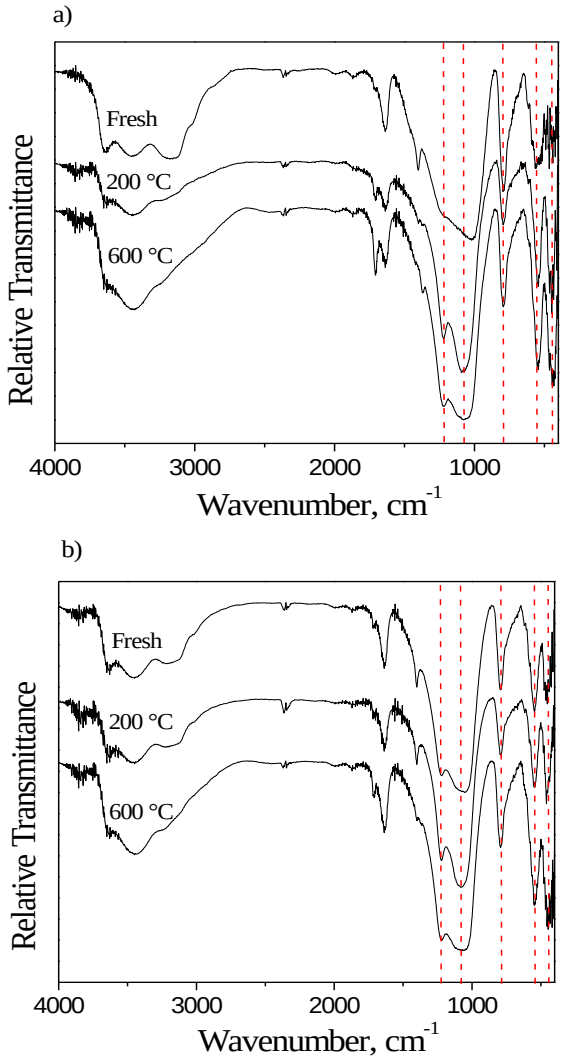

Figure 2. FT-IR spectra of the a) Cu(0.2%) and b) Cu(2%)ZSM5 zeolites, for the fresh sample, and after SCR reaction at 200 and 600 °C.

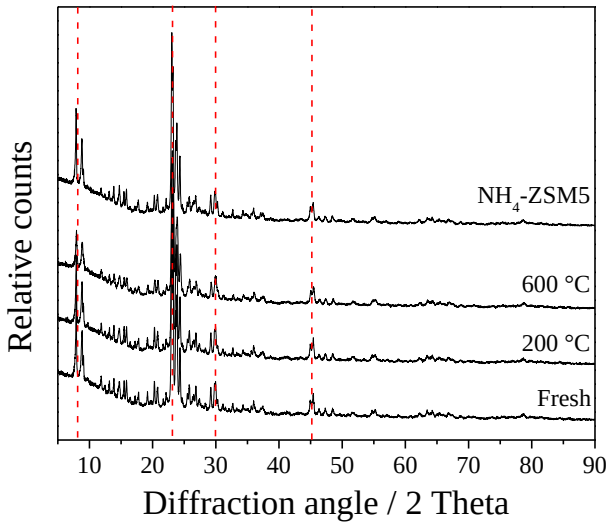

Figure 3. XRD patterns of the Cu(2%)ZSM5 sample, for the fresh catalyst and after SCR reaction at 200 ºC and 600 ºC. A comparison with a pure, unmodified NH_4-ZSM5 sample is also provided.

and the 800 cm^{-1} signal is due to the symmetrical stretching vibration of Si-O. The band at 545 cm^{-1} is characteristic of Si-O bonds in double rings of 5 members, while the band at 430 cm^{-1} is assigned to the internal Si/Al-O_4 tetrahedral bending bonds [34, 36].

Figure 3 shows the XRD results obtained for the fresh and used Cu(2%)ZSM5 catalyst, along with an XRD plot for the pure, unmodified NH_4-ZSM5. The defined and sharp peaks are proof of the full crystallinity of the catalysts. Characteristic NH_4-ZSM5 peaks can be observed (JCPDS 44-0002), specially at the diffraction angles of 7.94, 23.08, 30.04 and 45.35. Typical elemental copper signals have been reported to appear at 2θ values of 43.6°, while CuO peaks should be observed at 2θ = 35.7 and 38.6° [37, 38]. However, according to Figure 3, no sign of copper was found in the XRD analysis, with even the highest copper loading (2 %) showing identical 2θ peaks to that of pure, unmodified NH_4-ZSM5. This may indicate that the Cu phases are not fully developed or that the domains are too small to generate the periodicity needed for diffraction [28].

The results obtained from the UV-Visible spectroscopy analysis are summarized in Figure 4, for the zeolites modified with three different copper contents.

When transmittance or absorbance units are used to plot an UV-Visible spectrum, it is assumed that transmission sampling was used; however, since our analysis were performed using diffuse reflectance mode, we used the Kubelka-Munk units, which relate the intensity of diffused reflected light to concentration [39].

From Figure 4, some important discussions can be made. First of all, three characteristic UV-Vis signals attributed to Cu can be identified. All Cu-ZSM5 samples showed a band centered at 12,300-12,700 cm^{-1}, which has been related to the d-d transition occurring in typical isolated Cu^{2+} ions stabilized in octahedral crystal fields with small tetragonal distortion [40]. Another characteristic signal observed in all Cu-ZSM5 catalysts was the band at 47,000 cm^{-1}, which is related to a charge transfer (CT) O → Cu transition of isolated Cu^{2+} ions in coordination with lattice oxygens [41, 42]. Another absorption band at 25,500 cm^{-1} is observed, which has been identified with a ligand to metal charge transfer (LMCT) of copper oxide core clusters (axial or square-plane dimer) [43, 44]. All these copper species and interactions are adscribed to the decomposition of aqua complexes formed in the aqueous ion exchange (before calcination), which induce the removal of water from the first coordination sphere of Cu^{2+} [41]. In most cases, the general tendency of the copper-related UV-Vis bands was to increase in intensity with increasing content of metal in ZSM5, which is in agreement with the methodology followed. However, at higher SCR temperatures, the signal at 47,000 cm^{-1} tend to decrease in intensity (compared with the fresh catalysts). The signal at 25,500 cm^{-1}, on the other hand, keeps its intensity almost constant in all temperatures evaluated (except for the catalyst with 1 % Cu, where a decrease in the intensity is observed), which makes us conclude that although both Cu^{2+} forms are present(isolated copper and CuO), the latter are the most thermally stable form in the catalyst. Copper oxide

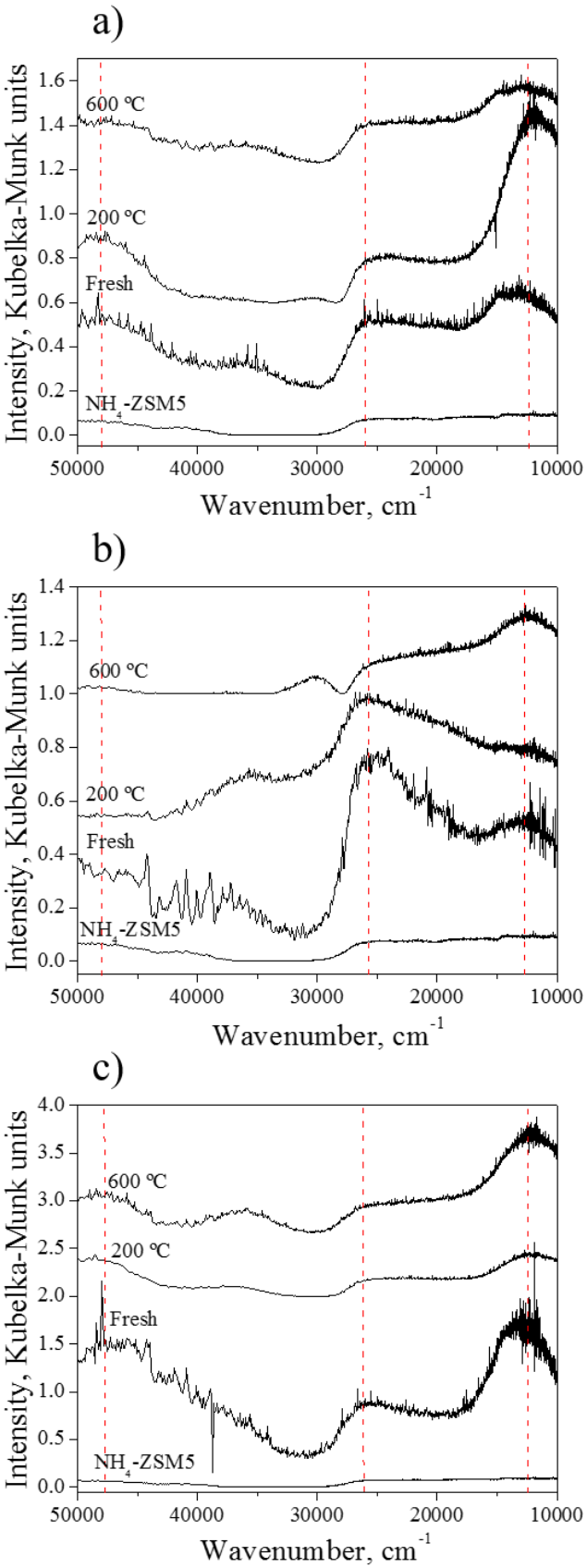

Figure 4. UV-Vis spectra for fresh and used Cu-ZSM5 catalysts: a) Cu(0.2%), b) Cu(1.0%), and c) Cu(2.0%). An unmodified NH_4-ZSM5 sample plot is provided in each plot for comparison.

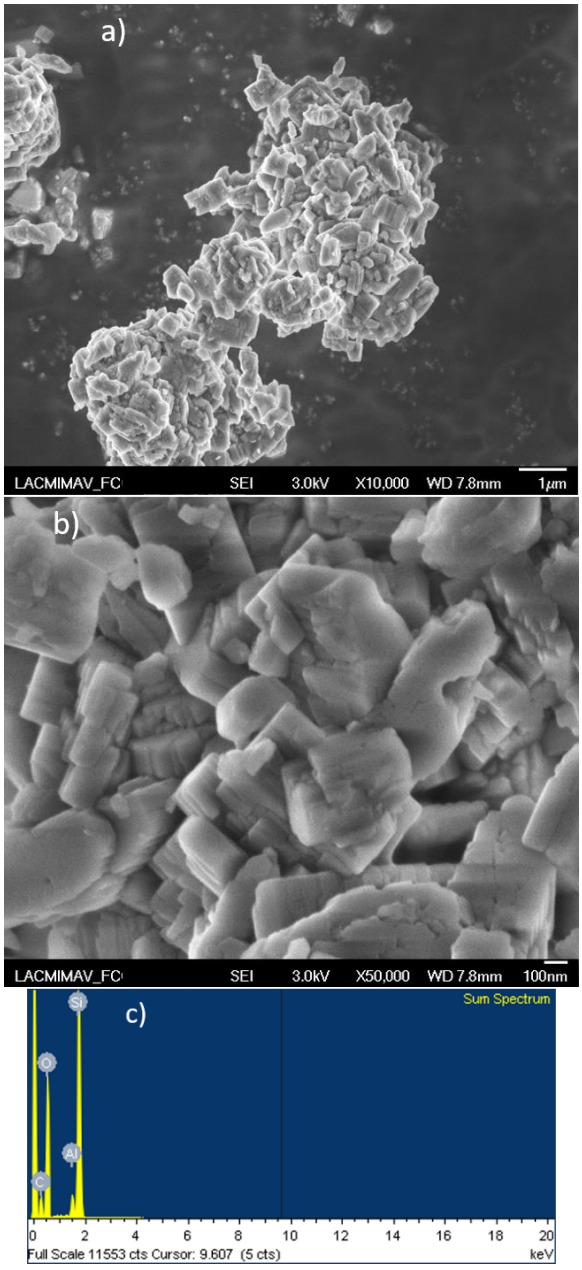

Figure 5. SEM characterization of the unmodified NH4-ZSM5 zeolite: a) micrograph with 1 μm resolution; b) micrograph with 100 nm resolution, and c) EDS spectrum.

cores have been associated with release of O_2 from the catalyst surface, which have been shown to promote NO decomposition and therefore a high activity of Cu-ZSM5 [44, 45]. This evidently explains the higher NO_x conversion results observed in Figure 1, where Cu(0.2%)ZSM5 did not match the other catalysts catalytic activity due to lack of enough copper oxide cores.

In order to evaluate the general zeolite morphology and the presence of copper in the catalyst, and to analyze the difference on this material before and after copper modification by aqueous ion exchange, NH4-ZSM5 and Cu(2%)ZSM5 samples were analyzed by SEM and EDS.

The results are resumed in Figures 5 and 6.

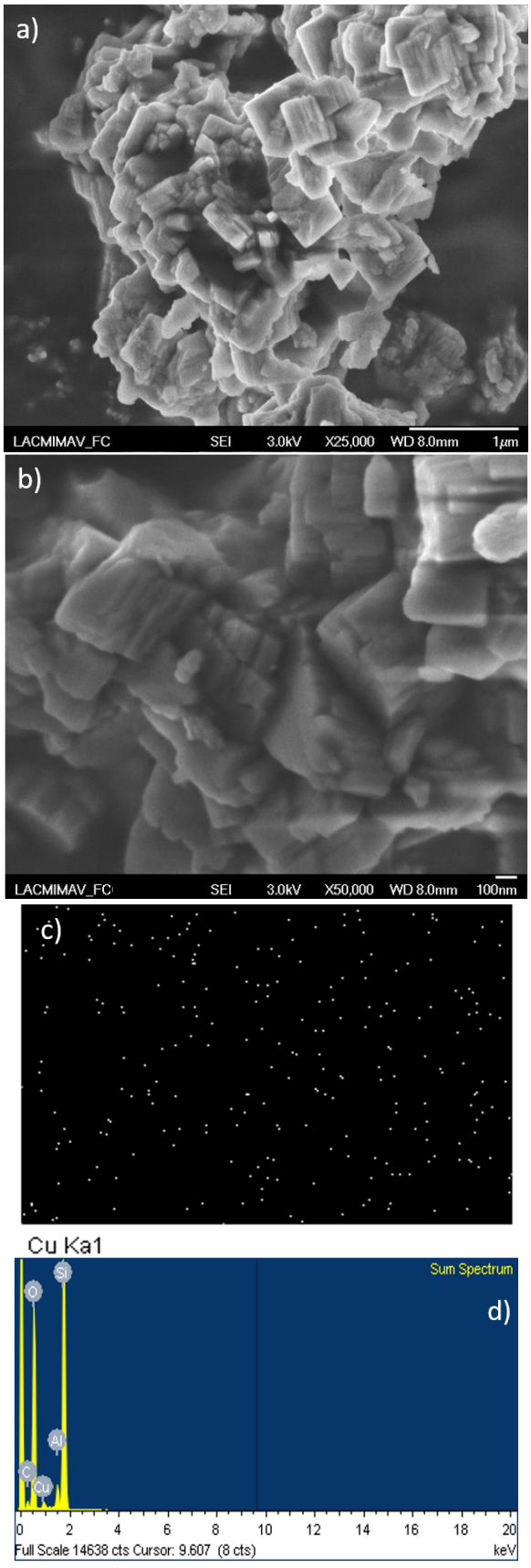

Figure 6. SEM characterization of Cu(2%)ZSM5: a) micrograph with 1 μm resolution; b) micrograph with 100 nm resolution, c) elemental Cu mapping over the catalyst, and d) EDS spectrum.

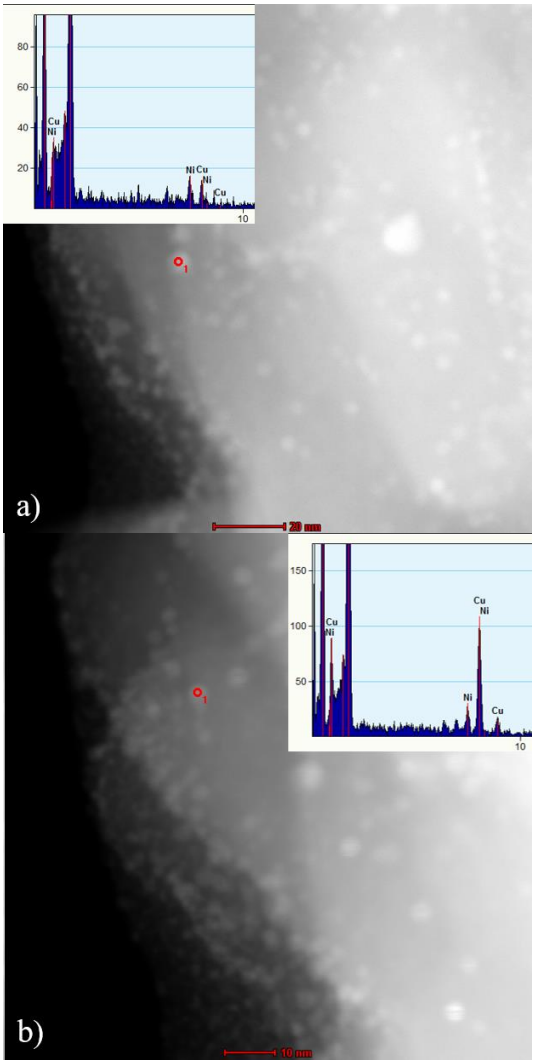

Figure 7. Characterization of fresh Cu(2%)ZSM5 by STEM, showing the EDS analysis over two different copper particles in the zeolite.

In these micrographs, it was observed that while unmodified NH_4-ZSM5 zeolite particles form agglomerates with a size of between 650 and 850 nm, the copper modification promotes a reduction in the agglomerate size, decreasing to between 300 and 450 nm. However, the crystal morphology remains unmodified, which agrees with previous studies on this materials [46, 47]

Clear Cu signals can be observed in EDS, at approximately 0.95 and 8.10 keV (Figure 6d) for the Cu(2%)ZSM5 catalyst. This signals are absent on the unmodified NH4-ZSM5 zeolite (Figure 5c). Elemental mapping of Cu shows absence of copper particle agglomerations, which confirms high dispersion over the ZSM5 zeolite (Figure 6c).

The results obtained from STEM and spot EDS analysis of the Cu(1%)ZSM5 fresh catalyst are found in Figure 7.

STEM images were taken to examine the morphology of Cu species and the support (ZSM5). Zeolite channels were observed from the STEM micrographs. Spherical copper particles (copper oxides, as discussed from the UV-Visible results) are observed, which confirm the copper modification of the zeolites. To discuss if the particles are inside or outside

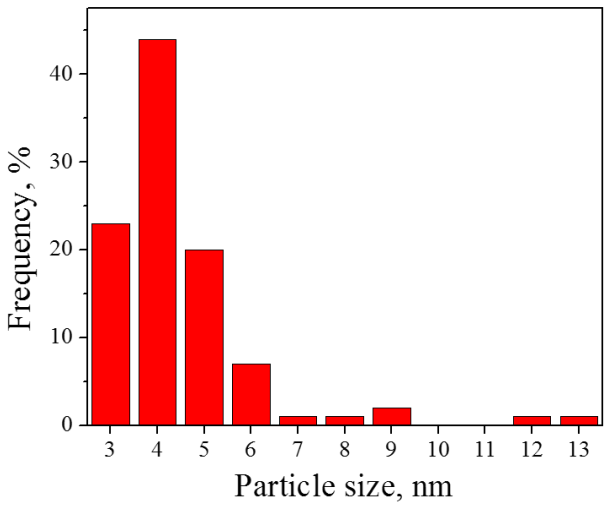

Figure 8. Particle size distribution analysis from fresh Cu(1%)ZSM5.

the channels, EDS was performed over two spots representing two different Cu particles over the same area. Though both particles show a copper signal on the EDS analysis, Figure 7a shows a very weak Cu intensity, while Figure 7b shows a more prominent signal. This may be an evidence to show the presence of Cu particles both inside the zeolitic channels (weak EDS signals) and over the surface of the ZSM5 (strong EDS signals).

An apparent uniform dispersion can be observed from the STEM images. The particle size distribution analysis (calculated using the TIA software provided by FEI on the STEM micrographs) in Figure 8 appears to confirm this assumption, due to the main predominance of 4 nm particles, instead of bigger aggregates, which have been previously shown to have sizes between 15 and 30 nm [48, 49]. However, some degree of heterogeneity between particle sizes is also observed, with 13 nm being the biggest particle size present in the zeolite.

HR-TEM was performed over the Cu(2%)ZSM5 sample in order to have a better understanding of the crystallinity and nature of the copper particles. The results are shown in Figure 9. Copper particles with different sizes are again observed, and an increase in image resolution (Figure 9b) showed evident crystal planes corresponding to copper species, likely the CuO species observed in the UV-Visible studies.

Conclusions

Zeolite supports were successfully modified with low contents of copper; the zeolites modified with 1.0 and 2.0 % of this metal showed a remarkable NO_x reduction performance (with 90-100 % conversion above 500 ºC), even when compared with other studies where the copper content was greater (almost 3 %).

The presence of Brönsted acid sites and copper oxides was confirmed by FT-IR and UV-Vis, respectively, which enhance the SCR activity of the catalyst. Isolated Cu^{2+} species were also found, but these are not thermally stable

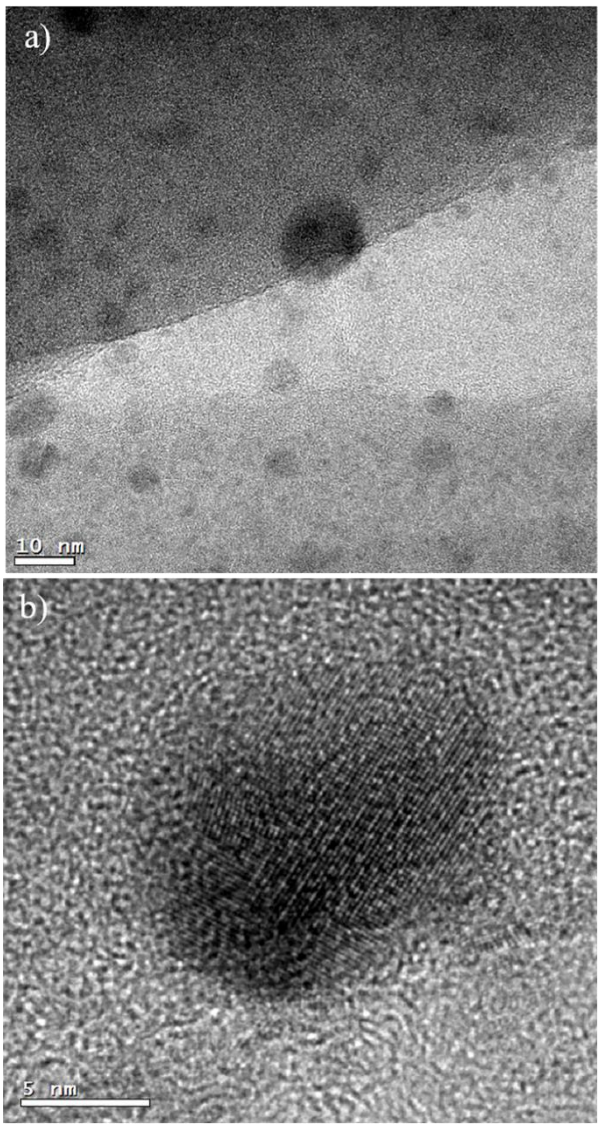

Figure 9. HR-TEM characterization of Cu(2%)ZSM5: a) micrograph with 10 nm resolution, b) micrograph with 5 nm resolution.

and therefore by 200 ºC are almost gone; on the other hand, copper oxides showed high stability. Copper XRD signals were not found, probably due to lack of Cu phase development, small domain size or high particle dispersion.

The aqueous ion exchange method allowed the formation of spherical particles, which were analyzed using SEM and STEM and were visually found to be dispersed over the ZSM5 catalyst using elemental mapping. A particle size distribution analysis shows copper cores are only 4 nm in size, which is small compared to other previous works, and also may suggest the lack of agglomeration and, in the contrary, the presence of highly dispersed particles. The high and apparently homogeneous copper particle dispersion may also contribute to the high NO_x conversion performance of these materials.

Aknowledgements

We would like to acknowledge CONACYT and Fundación UANL for the respective grants provided.

References

[1]. B.M. Belzowski, P. Green, *Total Cost of Ownership: A Gas Versus Diesel Comparison* (University of Michigan Transportation Research Institute, 2013).
[2]. E. Kates, W. Luck. *Motores diesel y de gas de alta compresión*, 2nd Ed. (Editorial Reverté, 2003).
[3]. Self Study Programme 230: Motor vehicle exhaust emissions (Volkswagen AG, Wolfsburg, 2012).
[4]. M. Votsmeier, T. Kreuzer, J. Gieshoff, G. Lepperhoff, in: *Ullmann's Encyclopedia of Industrial Chemistry*, 6th Ed. (John Wiley & Sons, 2012).
[5]. P. Crutzen. *Annu. Rev. Earth Pl. Sc.* **7**, 443 (1979).
[6]. T. Ryerson, M. Trainer, W. Angevine, C. Brock, R. Dissly, F. Fehsenfeld, G. Frost, P. Goldan, J. Holloway, G. Hübler, R. Jakoubek, W. Kuster, J. Neuman, D. Nicks, D. Parrish, J. Roberts, D. Sueper, E. Atlas, S. Donnelly, F. Flocke, A. Fried, W. Potter, W. Schauffler, V. Stroud, A. Weinheimer, B. Wert, C. Wiedinmyer, R. Alvarez, R. Banta, L. Darby, C. Senff, *J. Geophys. Res. Atmos.* **108**, 4249 (2003).
[7]. J. Calvert, W. Stockwell, *Environ. Sci. Technol.* **17**, 428 (1983).
[8]. J. Ibanez, K. Rajeshwar, in: *Encycl. Applied electrochem.*, 1st Ed., Eds: G. Kreysa, K. Ota, R. Savinell (Springer-Verlag New York, 2014).
[9]. D. Lewis, J. Mama, J. Hawkes, *Materials* **6**, 517 (2013).
[10]. G.W. Schade, P.J. Crutzen, *J. Atmos. Chem.* **22**, 319 (1995).
[11]. *Cuarto almanaque de datos y tendencias de la calidad del aire en 20 ciudades mexicanas (2000-2009)* (Instituto Nacional de Ecología y Cambio Climático de México, 2011).
[12]. C. García-Robles, *Master's Thesis* (UNAM, 2010).
[13]. *Inventario de emisiones contaminantes y de efecto invernadero, Zona Metropolitana del Valle de México 2012* (Secretaría de Medio Ambiente de la Ciudad de México, México, D.F., 2013).
[14]. T. Céspedes-Clavijo, *Master's Thesis* (ITESM, 2014).
[15]. P. Granger, V. Parvulescu, *Catal. Rev.* **111**, 3155 (2011).
[16]. Norma Oficial Mexicana NOM-042-SEMARNAT-2003 (Secretaría del Medio Ambiente y Recursos Naturales, México, 2005).
[17]. Y. Mao, H. Wang, P. Hu, *Int. J. Quantum Chem.* **115**, 618 (2014).
[18]. S. Brandenberger, O. Kröcher, A. Tissler, R. Althoff, *Catal. Rev.* **50**, 492 (2008).
[19]. M. Koebel, M. Elsener, M. Kleemann, *Catal. Today* **59**, 335 (2000).
[20]. X. Shi, F. Liu, L. Xie, W. Shan, H. He, *Environ. Sci. Technol.* **47**, 3293 (2013).
[21]. K. Rahkamaa, T. Maunula, M. Lomma, M. Huuhtanen, R. Keiski, *Catal. Today* **100**, 217 (2005).
[22]. X. Shang, J. Li, X. Yu, J. Chen, C. He, *Front. Chem. Sci. Eng.* **6**, 38 (2012).
[23]. A. Beale, I. Lezcano, T. Maunula, R. Palgrave, *Catal. Struct. React.* **1**, 25 (2015).
[24]. J. Hoej, M. Beier, *SAE Int J. Engines* **7**, 1397 (2014).
[25]. Z. Liu, N. Ottinger, C. Cremeens, *Atmos. Environ.* **104**, 154 (2015).
[26]. J. Li, H. Chang, L. Ma, J. Hao, R. Yang, *Catal. Today* **175**, 147 (2011).
[27]. M. Iwamoto, H. Furukawa, Y. Mine, F. Uemura, S. Mikuriya, S. Kagawa, *Chem. Commun.* **16**, 1272 (1986).
[28]. P. Vennestrom, T. Janssens, A. Kustov, M. Grill, A. Puig, L. Lundegaard, R. Tiruvalam, P. Concepción, A. Corma, *J. Catal.* **309**, 477 (2014).
[29]. G. Delahay, D. Valade, A. Guzman-Vargas, B. Coq, *Appl. Catal. B* **55**, 149 (2005).

[30]. S. Brandenberger, O. Kröcher, A. Tissler, R. Althoff, *Appl. Catal. B* **95**, 348 (2010).
[31]. S. Brandenberger, O. Kröcher, A. Tissler, R. Althoff, *Ind. Eng. Chem. Res.* **50**, 4308 (2011).
[32]. *Chemiluminescence NO-NO_2-NO_x Analyzer, Model 42i High Level* (Thermo Scientific, Franklin, USA 2007).
[33]. C. Pazé, S. Bordiga, C. Lamberti, M. Salvalaggio, A. Zecchina, *J. Phys. Chem. B* **101**, 4740 (1997).
[34]. P. Morales, J. Domínguez, L. Bucio, F. Álvarez, U. Sedran, M. Falco, *Catal. Today* **166**, 25 (2011).
[35]. R. Mohamed, H. Aly, M. El-Shahat, I. Ibrahim, *Micropor. Mesopor. Mat.* **79**, 7 (2005).
[36]. C. Leal, S. Gomez, C. Saux, L. Pierella, L. Pizzio, *Quim. Nova* **38**, 518 (2015).
[37]. J. Yan, G. Lei, W. Sachtler, H. Kung, *J. Catal.* **161**, 43 (1996).
[38]. J. Hun, D. Tran, S. Burton, J. Szanyi, J. Lee, C. Peden, *J. Catal.* **287**, 203 (2012).
[39]. L. Yang, B. Kruse, *J. Opt. Soc. Am. A* **21**, 1933 (2004).
[40]. S. Yashnik, Z. Ismagilov, V. Anufrienko, *Catal. Today* **110**, 310 (2005).
[41]. F. Giordanino, P. Vennesträm, L. Lundegaard, F. Stappen, S. Mossin, P. Beato, S. Bordiga, C. Lamberti, *Dalton Trans.* **42**, 12741 (2013).
[42]. S. Korhonen, D. Fickel, R. Lobo, B. Weckhuysen, A. Beale, *Chem. Commun.* **47**, 800 (2011).
[43]. A.B.P. Lever, *Inorganic Electron Spectroscopy*, 2nd Ed. (Elsevier, Amsterdam, 1984).
[44]. M. Groothaert, J. van Bokhoven, A. Battiston, B. Weckhuysen, R. Schoonheydt, *J. Am. Chem. Soc.* **125**, 7629 (2003).
[45]. Y. Li, W. Hall, *J. Catal.* **129**, 202 (1991).
[46]. E. Basaldella, A. Kikot, C. Quincoces, M. González, *Mater. Lett.* **51**, 289 (2001).
[47]. L. Shirazi, E. Jamshidi, M. Ghasemi, *Cryst. Res. Technol.* **43**, 1300 (2008)
[48]. Y. Zhang, M. Flytzani, *J. Catal.* **164**, 131 (1996).
[49]. L. Wang, W. Li, G. Qi, D. Weng, *J. Catal.* **289**, 21 (2012).